

TRANSPORT PROCESSES AND BUBBLE DRIVEN FLOW IN THE HALL-HÉROULT CELL

László I. KISS

Université du Québec à Chicoutimi, Chicoutimi, Québec, CANADA

ABSTRACT

The reaction zone in the aluminium electrolysis cell has a special geometry. While the length scale for the transport of the electric charge and metallic aluminium is only a few centimetres in the vertical direction, while the primary material, the alumina and the thermal energy need to traverse horizontal distances in the order of a meter. In this shallow, liquid filled reaction zone the horizontal convective loops play an important role in the homogenization of the intensive parameters like concentration and temperature. There are two important momentum sources present: the magneto-hydrodynamic and the buoyancy forces acting on the gas bubbles. The focus of the present paper is on the bubble-driven flow. While providing an important contribution to the horizontal mixing in the cell, the bubbles play a negative role by increasing the ohmic resistance and the energy consumption. A simulation method, based on the description of the behaviour of the individual bubbles was developed at UQAC. The bubble layer simulator follows the bubbles from the beginning of the nucleation through the detachment, coalescence etc. to the instant when they escape from the molten bath. The output of the method includes the covering factor, bath velocity under the anode, gas volume fraction, and bubble size distribution as functions of time. The influence of the design and operational parameters on the spectrum of the voltage fluctuations is also reproduced.

NOMENCLATURE

$F_D(v_j-v_i)$ drag force acting on or by the j th bubble
 $F_{VISC}(v_i)$ viscous resistance force acting on the i th associated mass
 m_i i th associated mass
 v velocity of the liquid layer under the anode
 v_i velocity of the i th associated mass
 v_j velocity of the j th bubble
 α advancing contact angle of a bubble
 β receding contact angle of a bubble
 $\Phi_i=v_i/v$ velocity ratio of the i th associated mass

INTRODUCTION

Although the Hall-Héroult process for the reduction of aluminium has been known for 120 years, the detailed quantitative description of the underlying physics and chemistry started to develop only with arrival of appropriate computing power and numerical methods in the past few decades. One of the first examples of the application of mathematical modelling to tackle reduction cell problems was the determination of the thickness and profile of the frozen sidewall ledge. Then, with the trend of increasing amperage, the need for a better

understanding and mastering of the magneto-hydrodynamic (MHD) effects arose. Beside the MHD forces, the other important source of momentum in the electrolysis cell is the buoyancy forces acting on the bubbles generated under the anode. On one hand these bubbles play an important, positive role by helping the homogenisation of the alumina distribution and the temperature field in the electrolyte. On the other hand they contribute to the increase of the ohmic overvoltage - that is to the increase of energy consumption - of the cell and they represent risks for the stable operation by perturbing the bath-metal interface and under certain conditions by provoking the so-called anode effects. The present paper deals with the mathematical modelling of the spatial structure and temporal fluctuations of the bubble-laden layer. The modelling approach is different from the general way CFD methods describe two-phase flows. Instead of working with the statistical average parameters that characterize a great number of disperse particles, the present method is based on the description of the bubbles individually, on a so-called "microscopic" level. This approach permits the computation of characteristics of the gas-liquid two-phase layer such as the detailed size distribution of the bubbles, its temporal fluctuations, the distribution of the bubbles along the anode bottom and the simulation of the voltage fluctuations as a function of the design and operational parameters of the cell etc.

TRANSPORT PROCESSES IN THE ALUMINIUM ELECTROLYSIS CELL

The basic features of the schema of the Hall-Héroult cell (or pot) have not changed much in the last hundred years (see Figure 1). The balance of the extensive properties includes the mass inputs of alumina and carbon, the electric charge and energy input while the outputs are the liquid aluminium, gases and thermal energy (heat), Figure 2. The solid alumina (Al_2O_3) is introduced vertically into the molten electrolyte (also called bath) either in the sidewall channels or between the anodes. It needs to be transported and distributed horizontally in the interelectrode space. The separation of the metallic aluminium and the evacuation of the gas produced by the electrolysis are done by gravity effects.

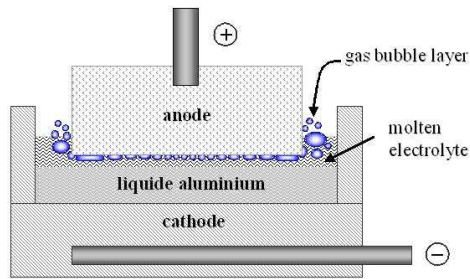


Figure 1: Schema of an aluminium electrolysis cell

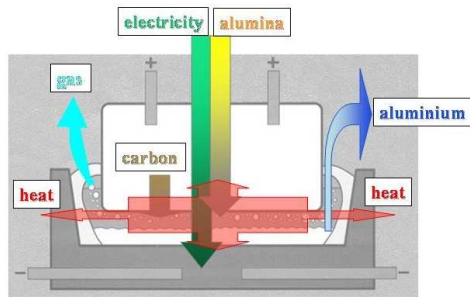


Figure 2: Mass, energy and electric flows in the cell

The geometry of the reaction zone in this electrochemical reactor is special: the electric charge and the metallic aluminium travels along a vertical distance of 4-5 centimetres only, while the alumina, the heat and the gases need to be transported horizontally to a distance about 20 times longer. The horizontal transport of mass and energy is very important to ensure optimal operation by homogenizing the intensive parameters (concentration, temperature). The mechanism of the horizontal transport is convection, driven by the MHD effects and by the bubbles. The bubbles play the role of a motor that converts gravitational energy into the kinetic energy of a horizontal movement. While convection in the horizontal plane is vital for the good operation of the cell, vertical convection is not welcome. Vertical movements either in the form of interface waves or turbulence in the very shallow electrolyte layer lead to negative effects such as reoxidation of the metallic aluminium, electric shortcuts etc. Minimizing the vertical movements, while promoting mixing in the horizontal plane, represents a great challenge for the design of the cells.

Bubble related phenomena in the reduction cell

Gas is generated under the anode and it forms a relatively thin (about 4-5mm, up to 10-12mm under dynamic conditions) bubble-laden layer. The bubbles escape around the edge of the anode, accelerating the liquid bath and inducing horizontal movement. The size of the loops of the bubble driven flow is in the order of the horizontal dimensions of the anode, while the other main source of momentum, the MHD effect creates loops on the length scale of the cell itself.

The gas under the anode restricts the passage of the electric current, increases the electric resistance and ultimately the energy consumption. The so-called anode effect is an extreme example when the gas blocks completely (or near completely) the bottom surface of the anode.

Length and time scales

One of the difficulties of modelling the transport phenomena in the electrolysis cell is related to the different length and time scales. Using the example of the bubble driven flow, the overall flow pattern exists on a length scale of about one meter, while the thickness of the bubble layer is about 200 times smaller. Many important details of the momentum exchange between bubbles and flow, and between bubbles and solid wall, can only be described correctly on the millimetre scale. (In order to describe the nucleation of a bubble one needs to descend to the micrometer scale, to the order of the pore sizes in the anode.) Another example is the distribution of the nucleation sites along the anode bottom. On the scale of the whole anode surface, one can say that gas is generated uniformly everywhere. However analysis of the distances between the neighbouring nucleation centres (the order is about a centimetre) shows very important differences due to the non-homogeneous structure of the aggregate material of the anode.

Considering the population of the gas bubbles under the anode, their size covers a range of about four orders of magnitude. Although the bubble related effects are dominated by the big bubbles, the dynamics of the morphological changes cannot be followed without consideration of the small ones.

Under steady state operation conditions, the rate of gas produced under the anode is equal to the rate of gas exiting from the bath. Under real operating conditions, this is true for the mean values averaged for a few seconds period, but the cell voltage shows fluctuations on the millisecond scale.

Gas covering and ohmic overvoltage

Although the production and evacuation rates of the gas are equal on an appropriately long time period, the quantity of the gas which stays under the anode in a given instant can vary widely. In chemical engineering this phenomena is generally characterized by the so-called gas-holdup rate i.e. by the volumetric ratio of the gas in the mixture. In aluminium electrolysis the covering factor – the gas covered portion of the anode bottom – is used very frequently, as it gives an indication about the resistance increase caused by the presence of the bubbles. However, the covering factor is directly linked only to one part of the resistance increase due to the bubbles, namely to the so-called screening effect, which is the result of the reduction of the electrically conducting section. The presence of the bubbles contributes to the resistance increase also by other mechanisms: they deform the originally homogeneous current density vector field and they shift the balance between the current passing through the bottom and sidewall of the anode.

MATHEMATICAL MODELING OF THE BUBBLE DRIVEN FLOW

The importance of modelling the bubble driven flow has been realized for a long time (Solheim et al., Chesonis and Lacamera, Purdie et al., Bilek et al.). The multiscale character of the transport phenomena in the reduction pot makes mathematical modelling difficult. Most of the CFD methods solve the flow problem for the continuous liquid phase and account for the disperse phase by using mean values (volume fractions, equivalent density, interface density etc.), statistical averages (mean diameter of the

bubbles) or quasi-continuum representations. This way, the details of the geometry and physical mechanisms on the level of individual bubbles are incorporated into these phenomenological, macroscopic values. The population dynamics can be followed by using empirical kinetic rates for the break-up and coalescence of the dispersed phase.

Microscopic modelling approach

As an alternative to the above mentioned methods, the so-called “microscopic” approach, based on the description of the evolution of every individual bubble as well as that of their interactions, was introduced. The basic ideas are common with those used in the modelling of “multi-agent” systems with a large number of interacting entities (see for example Czirók et al and Lerman et al). As in statistical mechanics, the behaviour of a grand ensemble of particles emerges from the description of the individual particles and interactions.

In the microscopic description, the life of a bubble is followed from the beginning of the nucleation through the growth at the nucleation site, detachment, movement, interactions with other bubbles, escape from below the anode, and vertical rise in the side-channel, just to the final escape at the upper free surface of the liquid. The continuous phase creates a link between the bubbles, as on one hand, the liquid is brought into motion by the bubbles and on the other hand, the liquid is acting on the bubbles by detaching them from the solid and by accelerating them.

The success of such an approach depends on the knowledge of the details of the underlying mechanisms, on the appropriate description of the physics of the interactions. For this reason, the development of the mathematical model started with the analysis of the evolution and movement of single bubbles and their interactions and finished with the development of a simulator that incorporates all that knowledge.

Evolution and movement of single bubbles

The life of a bubble in the molten electrolyte can be divided into different evolution periods, separated by rapid, nearly instantaneous events. Such events are: the beginning of a growth cycle, the detachment from the nucleation site, collisions (coalescence) with another bubble etc. The fundamental difference between the events and periods is in their time scale: the events have such a short duration that it seems to be instantaneous compared to the time scale of the periods.

Diffusion controlled growth

The period of growth of individual bubbles has a smooth and continuous character before detachment, except the relatively short initial latent period. The growth of the bubbles is controlled by diffusion. When the gas is stored in the liquid electrolyte (as it is the case in aqueous electrolytic systems) the volume-time history can be described analytically by a $3/2$ power law, Figure 3.

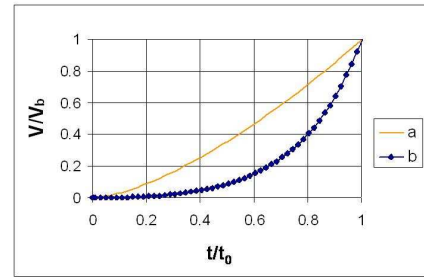


Figure 3: Diffusion controlled growth of bubbles: diffusion in the liquid (a), diffusion in the solid (b)

The character of the bubble growth in an aluminium reduction cell where the storage and transport of gas takes place in the porous anode is also shown in Figure 3, as it was obtained by numerical simulation (Poncsák 1999). For an easier comparison of their shapes, the two curves were normalized with the duration of the growth cycle and with the detachment volume. During the diffusion-controlled growth, the increase of the diameter of the bubbles covers 2-3 orders of magnitude, from a few micrometers to about half a centimetre. Correspondingly, the bubble volume increases several million times during this period. The t_0 period of the diffusion controlled growth is estimated to be somewhere between 100 and 400 milliseconds, depending on the design and operating conditions of the cell.

Detachment

The detachment is the event that separates two distinct periods of growth from each other. During the diffusion controlled period the bubble sits at the nucleation centre. It is continuously deformed under the action of buoyancy and hydrodynamic forces (Figure 4 and Figure 5). After detachment it is moving horizontally while separated from the anode bottom by a thin liquid layer, the so-called wetting film.

A bubble starts to move when it is not able to counterbalance the detachment forces by further deformation of its shape. Although the beginning of the movement is instantaneous, the formation of the wetting film takes a finite time. Under laboratory conditions with a single bubble in a water-air-plexiglass system with motionless liquid phase, the formation of the wetting film can take few seconds as shown in Figure 6 (Perron et al).

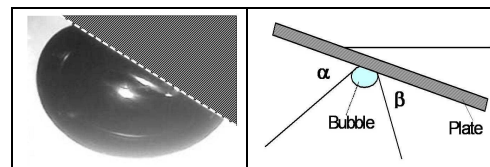


Figure 4: Detachment under an inclined anode bottom

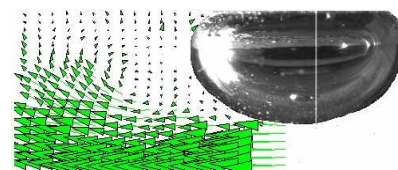


Figure 5: Detachment under the effect of liquid flow

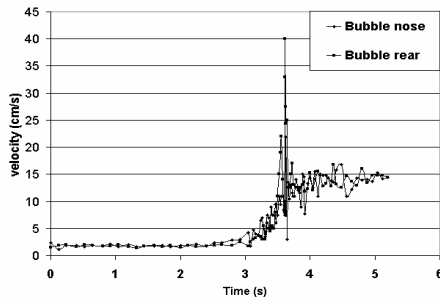


Figure 6: Variation of the bubble velocity after departure and during the formation of the wetting film (detachment)

However in a real electrolysis cell the strong flow fluctuations and surface inhomogeneities accelerate the formation of the wetting film, so the detachment can be considered as an instantaneous event.

Coalescence controlled growth

After detachment, the growth of the moving bubbles is basically controlled by coalescence. The law of growth is not continuous, as shown by the simulated curves in Figure 7; each sudden increase in bubble volume corresponds to a coalescence event.

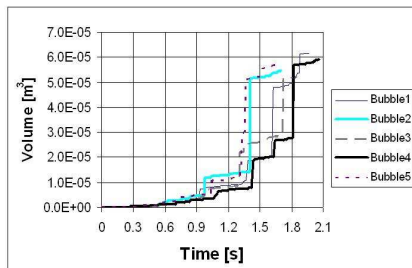


Figure 7: Coalescence controlled growth of five randomly selected bubbles

In the coalescence controlled period, the horizontal diameter of the bubbles increases about 20 times - depending on the anode size - but their volume increases only about 500 times, due to their flattened shape. After detachment, the volume of the bubbles increases mostly by spreading horizontally; the vertical dimension of the bubbles is practically constant.

There are several types of coalescence events depending on the relative size, position and approach velocity of the bubbles. The two most important coalescence classes are triggered by a collision due to velocity differences between two moving bubbles and by the contact between a moving bubble and a generally smaller, steady bubble during the diffusion controlled growth of the latter.

Collective behaviour of the bubbles

A schematic representation of the structure of the bubble layer - based on observation of low-temperature laboratory models - is given below (Figure 8).

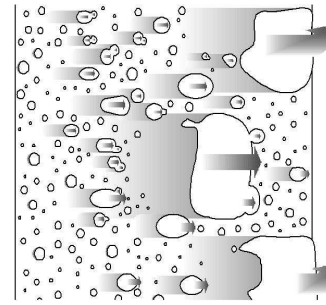


Figure 8: Schematic structure of the bubble layer

During movement of the bubbles, the covering factor fluctuates. The character of the fluctuations depends on many factors, but the number of the bubbles plays a very important role. In the case of one single bubble at a time under the anode, a regular, periodic temporal behaviour can be observed that corresponds to the individual growth law of the bubble (Figure 9). If there are many bubbles present, their combined effect on the covering factor generally results in a random-like fluctuation as shown in the second graph in Figure 9. However, under certain conditions, the bubbles can manifest a concerted movement (bottom graph in Figure 9). The formation of very big gas pockets and their sweeping action can trigger events like nucleation and a kind of "self-organization" occurs in the two-phase flow.

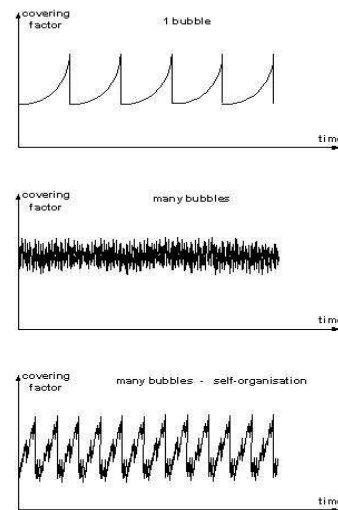


Figure 9: Character of the fluctuation of gas covering as a function of the number of bubbles

In our microscopic model, there is a one-to-one correspondence between the nucleation sites and elementary gas-generating surfaces, e.g. a surface element always feeds the same nucleation centre. An important issue that influences the temporal character of simulated voltage fluctuations is how the individual nucleation centres are arranged along the anode surface and how they are triggered. If the bubbles are generated in the nodes of a regular, uniformly spaced mesh and all of them start the nucleation cycle at the same instant, the fluctuations of the gas covered portion of the anode will be very regular, including a few harmonic oscillations. In reality, although the structure of the anodes is homogeneous on the centimetre scale ("meso-scale"), below that scale, on the millimetre and micrometer level ("micro-scale") there are large variations in the properties of grains and pores. To

reflect the effect of the real anode structure in the model, the meso-scale homogeneity was respected by tiling the anode surface with uniform elementary gas generating cells (Figure 10).

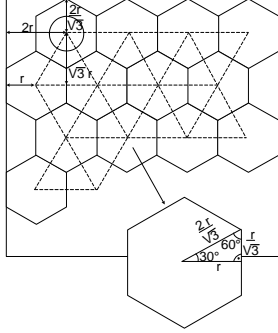


Figure 10: Mesh of the nucleation sites with hexagonal elements along the active anode surface

Square and hexagonal elements, like those shown in Figure 10, were chosen for the vast majority of the simulations. As in the real world, the nucleation sites are not aligned along straight lines like the dotted lines in Figure 10. The nucleation centres were randomly placed inside a circle around the nodes of the mesh. The diameter of the circle inside the elementary cell characterizes the scale of inhomogeneities in the anode. The diameter of the circle was chosen to respect a certain minimal distance between the neighbouring nucleation centres.

Momentum balance

In order to keep the bubble model computationally effective while keeping all the advantages of the microscopic approach (detailed morphology and dynamics), the flow calculation was simplified. The liquid velocities are computed by a lumped parameter approach. The flow domain is divided into individual entities like the bubble layer under the anode, rising bubbly column in the side-channel, sidewall vortex etc. These entities possess associated masses and characteristic (variable) velocities. The division is based both on experimental measurements on bubble-driven flow models and on numerical simulations of the flow field. The momentum balance is then written in the following form:

$$\sum_i \left(m_i \phi_i \frac{\Delta v_i}{\Delta t} \right) = \sum_i \sum_j (F_D(v_j - \phi_i v)) - \sum_i F_{visc}(\phi_i v)$$

The left side is the variation of the momentum of all the associated masses, while the right side is the resultant of the accelerating and decelerating forces due to the bubble-liquid interaction and the viscous dissipation in the liquid phase. As the position, velocity, size and shape of every bubble are available in the model, the variation of the associated liquid masses can be easily determined in each time step of the computation:

$$m_i = \rho_L \left[V_i - \sum_j V_j \right]$$

The first term on the right side of the balance equation can have different signs +/- depending on the velocity of the bubble relative to the liquid. Slowly moving or steady bubbles dampen the flow; only bubbles moving faster than the liquid accelerate it.

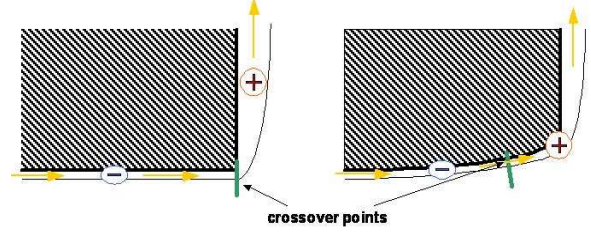


Figure 11: Schema of the momentum transfer between the bubbles and the liquid layer; flat, horizontal bottom (left) and the curved bottom of a used anode (right)

The change of the sign of the momentum exchange is shown schematically in Figure 11. The cross-over point is fixed to the anode corner in the case of a horizontal, flat bottom anode, while its position needs to be dynamically re-calculated at every time step in the case of a curved anode bottom.

The bubble layer simulator

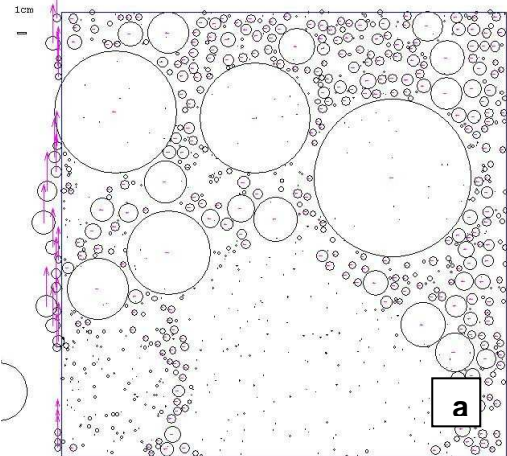
A bubble layer simulator has been built using the above outlined principles. It uses the design and operational parameters of a cell, like geometry, bath temperature, current density etc. as input parameters and by following the evolution of thousands of bubbles, determines the instantaneous and time averaged values of the gas-holdup, covering factor and bath velocity. The spatial distribution of the gas volume fraction and covering factor are also available as well as the bubble size distribution and a graphical representation of the morphology of the bubble layer. These data then can be used to determine the ohmic overvoltage by a separate calculation, without the need for hypothetical equivalent resistance models of the bubble layer.

RESULTS

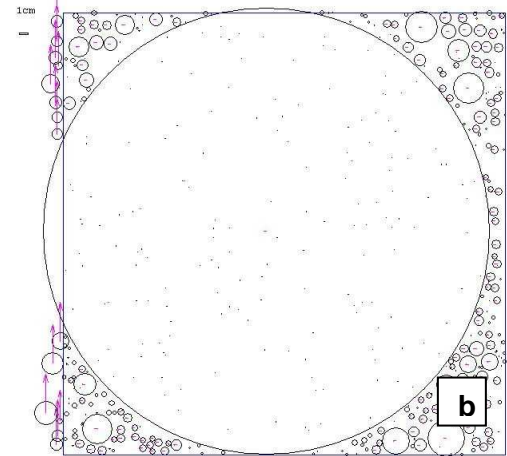
In Figure 12 we present three images of the bubble layer that were obtained by the mathematical model for industrial-size anodes. The images reflect well the intuitive expectations that under horizontal (new) anodes very big gas-pockets can be formed (first two images in Figure 12) and that even small inclination helps to reduce of the gas hold-up effectively.

The following results (Figure 13 and Figure 14) illustrate the effect of the length of travel of the bubbles along the anode surface. The shorter anode has a length of 10 units along the direction of the movement of the bubbles, while the longer one is 20 units long. The doubling of the length of travel affects the character of the fluctuations remarkably. The amplitude of both the covering factor and that of the velocity increases. The longer travel promotes the formation of big bubbles that abruptly accelerate the liquid layer during their escape and rise in the sidewall channel. This is why the sharp increase in the velocity coincides with the rapid decrease of the covering factor. The mean value of the covering factor also increases, while the mean velocity decreases, in harmony with the physical expectations. Furthermore, one can observe the emergence of a dominating, relatively low-frequency fluctuation in the case of the longer anode. As the big bubbles sweep along the anode surface they remove the smaller bubbles in their diffusion controlled growth phase at the nucleation centres. This way the big bubbles “synchronize” the beginning of the new nucleation cycles along the surface.

time : 19.00500 VERSION 5.3 - January 2006
 covering factor = 0.4130000
 velocity = 3.009206939372156E-002 total number of bubbles : 3730



time : 16.00500 VERSION 5.3 - January 2006
 covering factor = 0.8660001
 velocity = 3.015021577370686E-002 total number of bubbles : 3730



time : 15.00500 VERSION 5.3 - January 2006
 covering factor = 0.4400000
 velocity = 0.129764699316263 total number of bubbles : 6089

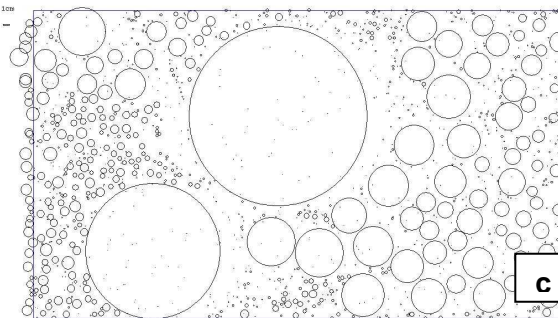


Figure 12: Bottom view of the computed bubble layer patterns for horizontal (**a** and **b**) at different instants and slightly inclined anodes (**c**); only half of the symmetrical horizontal anode (**a** and **b**) is shown (bubble movement is from right to left)

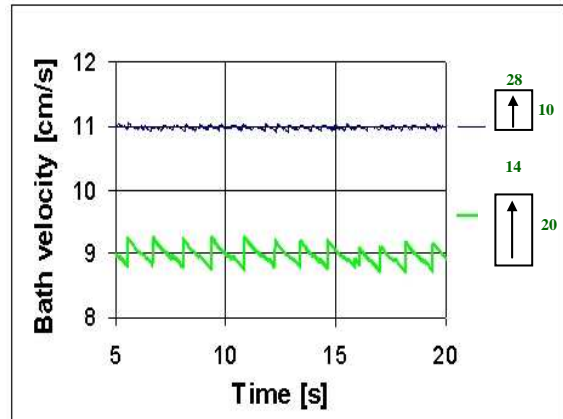
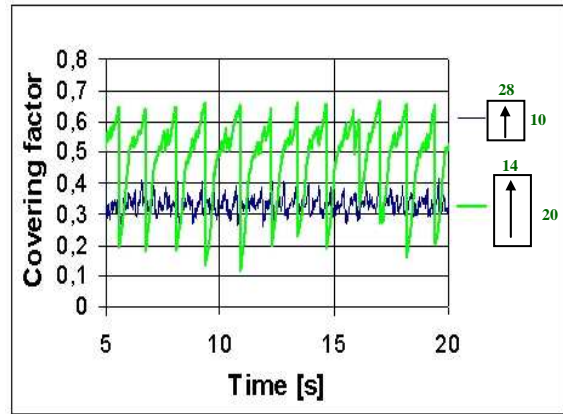


Figure 13: The effect of anode length on the fluctuations of the covering factor and bath velocity

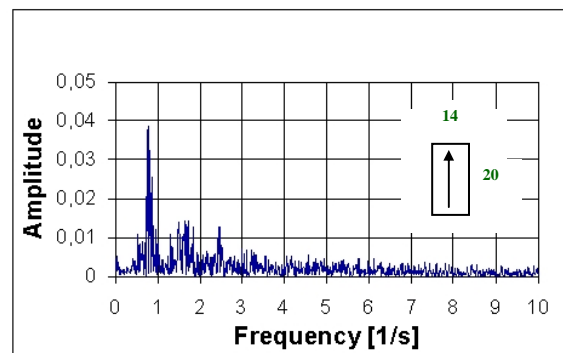
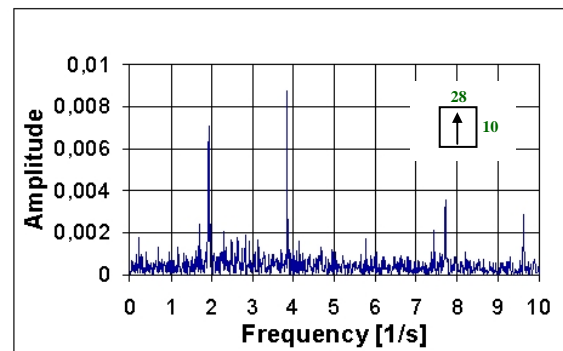


Figure 14: Spectrum of the voltage fluctuations for different anode lengths

These phenomena can also be illustrated by the spectrum of the covering factor and velocity fluctuations, as shown in Figure 14.

CONCLUSION

A mathematical model using a detailed description of the individual bubbles in the gas-liquid two-phase layer under a solid surface has been developed (so-called “microscopic” approach).

The primary application of the method is the analysis of the anodic overvoltage and its fluctuation in aluminium electrolysis cells.

The simulated fluctuations can also assist the interpretation of the measured voltage fluctuations, supporting the diagnosis of electrolysis cells.

ACKNOWLEDGEMENTS

The methods and results presented above reflect the work of a team. The list is too long to name all the collaborators here, so the author limits himself to underline the exceptional contributions of Sándor Poncsák and Alexandre Perron.

REFERENCES

BILEK M.M., ZHANG W.D., STEVENS F.J., (1994), Modelling of electrolyte flow and its related transport processes in aluminium reduction cells, TMS Light Metals, pp. 323-331.

CHESONIS D. C. and LACAMERA, A. F. (1990), The Influence of Gas-Driven Circulation on Alumina Distribution and Interface Motion in a Hall-Héroult Cell, TMS Light Metals, pp. 211-220.

CZIRÓK A, VICSEK T., (1999), Collective Motion; in Lecture Notes in Physics, proceedings of the XV Sitges Conference, Springer.

KISS, L. I., PONCSÁK, S. (2002), Effect of the bubble growth mechanism on the spectrum of voltage fluctuations in the reduction cell, TMS Light Metals, pp. 139-145.

LERMAN K, GALSTYAN A, HOGG T., (2004), Mathematical Analysis of Multi-Agent Systems, arXiv:cs.RO/0404002 v1.

PERRON A., KISS L., PONCSÁK S., (2005), Regimes of the Movement of Bubbles under the Anode in an Aluminium Electrolysis Cell, TMS Light Metals, pp. 531-537.

PONCSÁK S, KISS L, TOULOUSE D, PERRON A., (2006), Size distribution of the bubbles in the Hall-Héroult cells, TMS Light Metals, pp. 462-469.

PURDIE J.M., BILEK M., TAYLOR M.P., ZHANG W.D., WELCH B.J., CHEN J.J.J., (1993), Impact of anode gas evolution on electrolyte flow and mixing in aluminium eletrowinning cells, TMS Light Metals pp. 355-360.

SOLHEIM, A., JOHANSEN, S., ROLSETH, S. and THONSTAD, J. (1989), Gas Driven Flow in Hall-Héroult Cells, TMS Light Metals, pp. 245-252.